ACS Macro Letters

Letter

pubs.acs.org/macroletters

Distortion of Chain Conformation and Reduced Entanglement in Polymer–Graphene Oxide Nanocomposites

M. P. Weir,[*,†,∥] D. W. Johnson,[‡,∥] S. C. Boothroyd,[‡,∥] R. C. Savage,[†] R. L. Thompson,[‡] S. M. King,[§] S. E. Rogers,[§] K. S. Coleman,[‡] and N. Clarke[†]

[†]Department of Physics and Astronomy, The University of Sheffield, Hicks Building, Hounsfield Road, Sheffield S3 7RH, United Kingdom

[‡]Department of Chemistry, University of Durham, Durham DH1 3LE, United Kingdom

[§]ISIS Pulsed Neutron and Muon Source, Science and Technology Facilities Council, Rutherford Appleton Laboratory, Harwell, Oxford, Didcot OX11 0QX, United Kingdom

Supporting Information

ABSTRACT: We study the conformations of polymer chains in polymer–graphene oxide nanocomposites. We show that the chains have a reduced radius of gyration that is consistent with confinement at a solid interface in the melt, as is expected for well-dispersed, high aspect ratio nanoparticles that are much larger than the polymer coil size. We show that confinement of the polymer chains causes a corresponding reduction in interchain entanglements, and we calculate a contribution to the plateau modulus from the distorted polymer network via a simple scaling argument. Our results are a significant step forward in understanding how two-dimensional nanoparticles affect global material properties at low loadings.

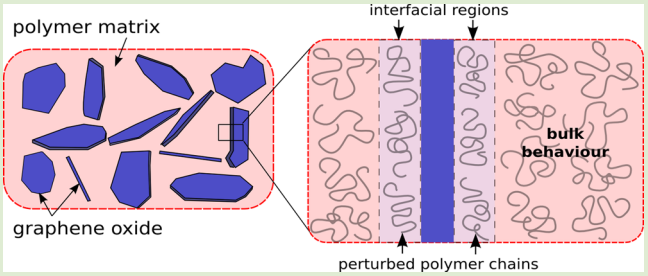

Graphene and related 2D materials have extraordinary physical properties that along with their high aspect ratio make them excellent candidate filler materials for polymer nanocomposites,[1] capable of producing significant gains in material properties at extremely low concentrations on the order of 1% by volume.[2,3] The conformation of polymer chains in the interfacial regions in the vicinity of nanoparticles is of great interest. The modified structure and dynamics of the chains in this region may have a significant role in determining the final properties of the composites. The effect of zero- and one-dimensional fillers upon the polymer chain dimensions has been well studied,[4−6] but the question of the effect of two-dimensional nanomaterials remains outstanding. In order to answer this problem, we investigate the effect of graphene oxide (GO), a highly functionalized form of graphene, upon the conformation of well-studied polymers poly(methyl methacrylate) (PMMA), where the GO is well-dispersed, and polystyrene (PS), where the GO dispersion is poor. We prepare the samples with a well-controlled thermal history, representative of typical industrial processing conditions. Using small-angle neutron scattering (SANS), we measure distortions in the polymer chain dimensions that show a distinct minimum in polymer chain dimensions at approximately 0.5% by volume of GO. Using rheology, we show that the distorted polymer chains, which each occupy less volume due to their confinement, are also less entangled with their neighbors, thus producing global changes to the sample behavior arising from nanometer-scale chain confinement. We present a direct measure of the effect of the GO upon the polymer matrix that relates to the bulk properties of the entire macroscopic composite material. We present a simple scaling analysis showing that the reduction in entanglement measured by rheology is associated with a reduction in chain dimensions, which is confirmed independently by the SANS measurements. This work significantly advances our understanding of the mechanisms by which nanocomposite material properties are modified by the presence of the filler.

Graphene oxide was exfoliated from graphite oxide[7] yielding nanoparticles with typical lateral dimensions of 5 μm and thickness of 1 nm, before polymer–graphene oxide (GO) nanocomposite samples were prepared by solvent processing in dimethylformamide (DMF) followed by compression molding (see Supporting Information for further details). Composites were formed of GO with poly(methyl methacrylate) and polystyrene, where each polymer matrix was formed from a blend of hydrogenous and deuterated polymer of closely matching molecular weight and polydispersity (dPMMA M_n = 234 kDa, PDI 1.14; hPMMA M_n = 237 kDa PDI 1.16; dPS M_n = 87 kDa, PDI 1.1; hPS M_n = 98 kDa, PDI 1.07) in order to highlight the individual chain conformations for SANS measurements.

Received: February 3, 2016
Accepted: March 8, 2016
Published: March 9, 2016

DOI: 10.1021/acsmacrolett.6b00100
ACS Macro Lett. 2016, 5, 430−434

SANS was carried out on the Sans2d instrument at the ISIS Pulsed Neutron Source (STFC Rutherford Appleton Laboratory, Didcot, U.K.).[7,8] The fitting function applied within the SasView software comprises a model for the radius of gyration (R_g) scattering of a Gaussian polymer coil recast with a Schulz–Zimm polydispersity function,[9] an absolute power law describing the GO scattering, and a constant background term, with the overall expression

$$I(q) = A\frac{2[(1+Ux)^{-1/U} + x - 1]}{(1+U)x^2} + Bq^{\alpha} + C \quad (1)$$

where A is a factor dependent on the volume fraction of deuterated polymer in the blend; x is the dimensionless substitution $x = \frac{R_g^2 q^2}{1+2U}$; and U is related to the polydispersity as $U = \frac{M_w}{M_n} - 1$. The obtained fitting parameters A, B, α, and C are tabulated in the Supporting Information.

The polymer R_g was measured from the fits to the SANS data as a function of GO nanoparticle concentration (Figure 1(a) and (b)). For poly(methyl methacrylate) (Figure 1(c)), a reduction in the polymer R_g is observed with increasing concentration between 0.02 and 0.5 vol %, with R_g reducing to 88% of its original value.

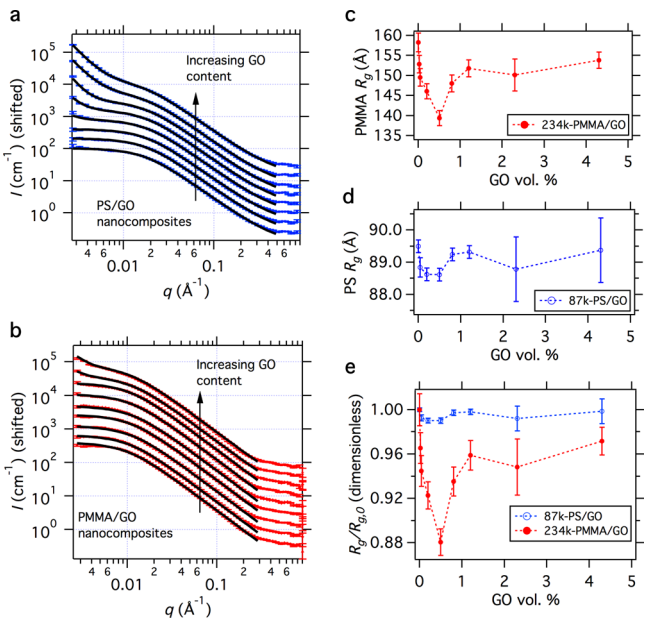

Figure 1. Extraction of R_g as a function of GO concentration from small-angle neutron scattering (SANS) data. SANS data (markers) and associated fits (solid lines) for (a) PS/GO and (b) PMMA/GO nanocomposites. (c,d) The radius of gyration (R_g) extracted from the data fits for PMMA/GO (c) and PS/GO (d) where error bars are the uncertainties in the fit. For PMMA/GO the polymer R_g exhibits a sharp minimum at a critical GO concentration. (e) R_g values normalized to the bulk value $R_{g,0}$.

A reduction in entanglement density has been observed by experiment and theory in various confinement geometries.[10−15] The dimensions of the filler nanoparticle and its relation to polymer chain size are of great importance.[16] High aspect ratio nanoparticles, and nanoparticles with size much greater than R_g, prevent chains within the vicinity of the surface from adopting a random coil conformation. Specific chemical interactions between the chain monomers and the nanoparticle surfaces also alter the chain conformation and dynamics.[17] Within an interfacial region extending one polymer R_g from the confining surface,[12,18] there is a predicted reduction in the component of R_g normal to the surface. Thus, for a good dispersion, the volume fraction of sample occupied by the interfacial volume surrounding the filler may be estimated using the specific surface area of the filler and R_g using the form $\phi_i = \phi_f S \rho_f R_g$. A theoretical specific surface area[19] of approximately $S = 2630$ m^2/g is predicted for pristine, perfectly dispersed graphene. Assuming this value for S, $\rho = 2.1$ g cm^{-3}, and using for example PMMA with $M_n = 234$ kDa and R_g of 16 nm, the volume fraction ϕ_i occupied by interfacial polymer chains is greater than 50 vol % for a filler volume fraction of ∼0.6 vol %, and $\phi_i \gg \phi_f$. The interfacial volume fraction ϕ_i increases with molecular weight in proportion to R_g. The quantity $\phi_{f+i} = \phi_f + \phi_i$ is most useful as it takes both filler and interface into account. Aside from purely steric effects, surface adsorption of the polymer at the GO interface could play an important role in the nature of the interfacial polymer layer. Although the largest reduction in R_g is expected in the direction normal to the surface,[12] a typically prepared nanocomposite sample has nanoparticles situated in all orientations. The powerful averaging of SANS thus allows the measurement of a global average of R_g for the sample, i.e., the average of the interfacial regions and the bulk, while rheological measurements probe the overall mechanical response of the sample and so are equally indiscriminate of chain orientation. It should be noted, therefore, that the interpretation presented in this paper yields only an average of interfacial and bulk chain conformations and relies on the basic assumption that the interfacial chain conformation could only be fully decoupled from the bulk chain conformation if the volume fraction of interfacial chains was precisely known or alternately if the interfacial chains could be explicitly labeled (say, via selective deuteration).

Rheology was performed on the actual SANS samples (after SANS) to ensure identical preparation and thermal history (for further details and discussion see Supporting Information). The time temperature superposition (TTS) theory of Williams–Landel–Ferry[20] was applied using the RepTate program.[21] The plateau modulus was determined by taking the value of the storage modulus, G', at the minimum of the phase shift angle within the plateau region. A power law model for the nanoparticle percolation of the GO within the composite can be applied by the relation[22,23]

$$G' \propto (\phi_f - \phi_{perc})^{\nu} \quad (2)$$

where ϕ_f is the volume fraction of GO; ϕ_{perc} is the percolation threshold of the GO in the composite; and ν is the exponent of the system. Fits to the two regimes are shown in the inset of Figure 3(c).

The plateau modulus attributed to the rubbery network of entangled polymer chains within a polymer melt is expressed as[24,25]

$$G_N^0 = \frac{4}{5}\frac{\rho RT}{M_e} \quad (3)$$

(where ρ is the monomer density, R the ideal gas constant). The minimum in R_g observed by the SANS experiments is reflected by a reduction in G_N^0 as a function of the GO concentration and is consistent with a decrease in interchain entanglements that results from the reduction in the configura-

DOI: 10.1021/acsmacrolett.6b00100
ACS Macro Lett. 2016, 5, 430−434

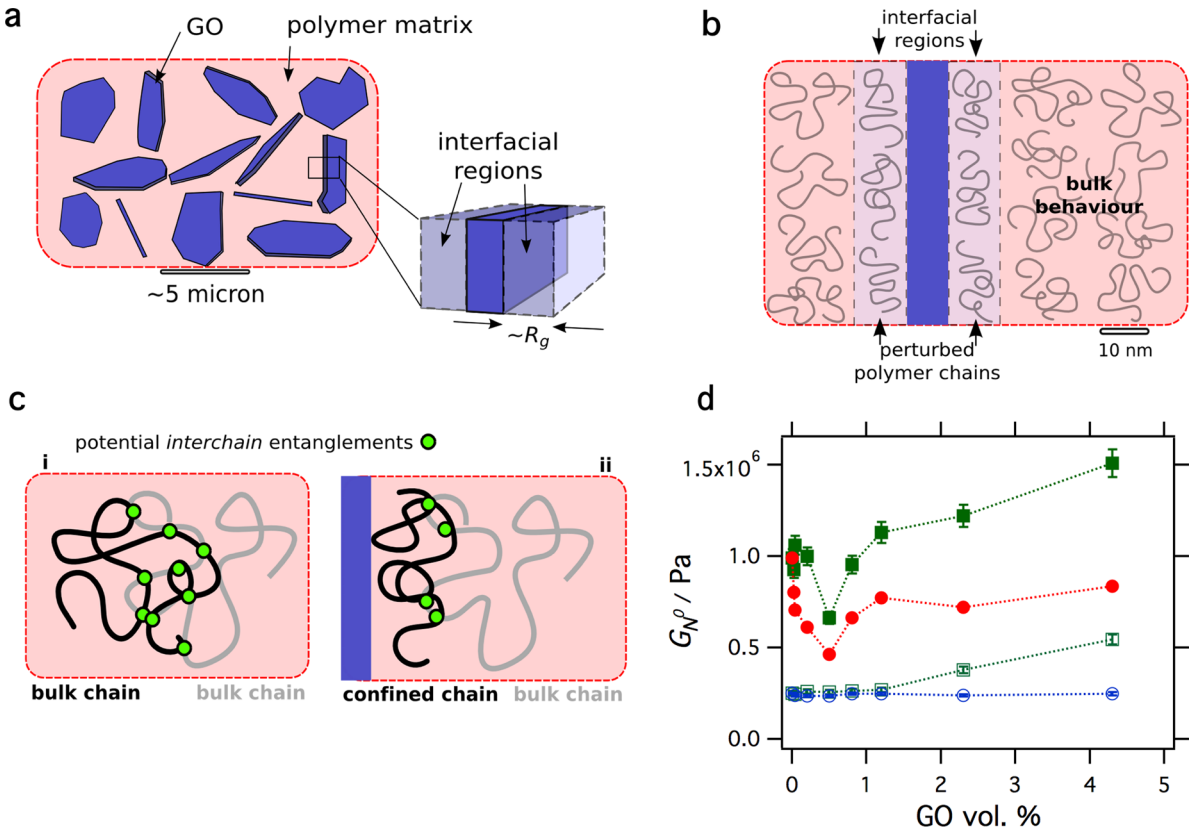

Figure 2. Illustrations of the interfacial regions in polymer−GO nanocomposites and the effect upon the plateau modulus as measured with SANS and rheology. (a) A schematic illustration of the effect of the interface of a high aspect ratio nanoparticle, such as GO, upon the single-chain conformation within a polymer melt. (b) A schematic diagram showing that within the interfacial regions the component of the polymer chain R_g normal to the surface is decreased, and this region is understood to extend approximately a distance of approximately one (bulk) R_g from the interface. (c) The potential for entanglements between a confined chain and the adjoining bulk chains is reduced since the chain occupies a reduced volume, meaning fewer encroachments from neighboring chains. (d) Plateau moduli as a function of GO concentration for 234k-PMMA/GO composites (filled symbols) and 87k-PS/GO composites (open symbols), measured using oscillatory rheology (squares) and calculated from SANS (circles).

tional volume available to the interfacial chains, as illustrated schematically in Figure 2 panels (a) to (c).

Brown and Russell[26] first considered the effect of the confining geometry of a flat, solid surface upon the polymer M_e. The total conformational volume pervaded by a Gaussian polymer chain[11,26] is given by

$$V_P = AR_g^3 = A'(M/m)^{3/2}a^3 \quad (4)$$

where M is the polymer molecular weight; m is the segment molecular weight; and a is the segment size, while the chain occupies a hard-core volume of $V_C = \left(\frac{M}{m}\right)a^3$. The ratio V_P/V_C gives a measure of the overlap between neighboring chains and is set to a constant (with a typical value of 2, depending upon chain packing,[11] the original model for which was proposed by Lin[27] and validated for a broad range of systems including PS and PMMA by Fetters and co-workers[28]) as a definition of M_e. This ratio is given by

$$\frac{V_P}{V_C} = A'(M_e/m)^{1/2} = B \quad (5)$$

and leads to the relation

$$M_e = m(B/A')^2 \quad (6)$$

Brown and Russell[26] proposed that if the dimensions of the chain were approximately halved near to an interface (equivalent in the current notation to setting $A' = 1/2$), this would produce a 4-fold increase in M_e. The effect upon the plateau modulus in the case of an unfilled polymer melt follows via eq 3. Using $R_g^3 = V_P/A$ as a measure of average polymer chain volume therefore allows us to track the perturbations to the polymer chain volume

$$A'/A'_0 = R_g^3/R_{g,0}^3 \quad (7)$$

We therefore calculate a scaled plateau modulus $G^0_{N,SANS}$ for the polymer network perturbed by the presence of GO *but not including the filler contribution*

$$G^0_{N,SANS}(\phi) = G^0_{N,0}(A'/A'_0)^2 \quad (8)$$

where $G^0_{N,0}$ is the corresponding rheological measure of the unfilled pure polymer, where eq 3 is valid. This calculated plateau modulus is compared with the measured rheological plateau modulus in Figure 2(d) and reproduces the key feature for the well-dispersed PMMA/GO composites of a depression up to 0.5 vol % GO followed by recovery, with a correlation between $G^0_{N,SANS}$ and G^0_N. The correlation (see Supporting Information) between $G^0_{N,SANS}$ and G^0_N for the PMMA/GO nanocomposites shows that the distortions to the polymer matrix are consistent with confinement of melt chains at a solid

DOI: 10.1021/acsmacrolett.6b00100
ACS Macro Lett. 2016, 5, 430−434

interface. The rheological plateau modulus is therefore the sum of the calculated plateau modulus and a contribution from the interactions between the entanglement network and the filler. Such contributions to G_N^0 may arise from contacts between the polymer network and the filler acting as temporary cross-links on the time scales probed, e.g., via transient pinning[17] or otherwise.

Rheology was carried out on additional composites of GO with PMMA (87 kDa). In Figure 3(a), the storage (G') and loss (G'') moduli of pure 87k-PMMA and 87k-PMMA/0.48% GO composite are shown as a function of frequency, shifted to a single temperature of 200 °C using TTS theory.[20] Figure 3(b) shows G' in the terminal increasing with increasing concentration of GO within the composite. Figure 3(c) shows this change in G' as a function of GO concentration. Two regimes are apparent in the data that suggest a change in the quality of the dispersion of the GO between these two regions, such as aggregation of the GO. The plateau modulus as a function of GO concentration is seen in Figure 3(d). Such a nonmonotonic trend in the plateau modulus of the polymer has also been observed by Liu et al.[29] for composites of ultra high molecular weight polyethylenes with reduced graphene oxide nanosheets (rGONs) where the minimum was interpreted to correspond with the rGON concentration value that gave the most efficient dispersion, before aggregation effects began to reduce the surface area to volume ratio (hence reducing the available polymer−rGON interactions) and increase the storage modulus.

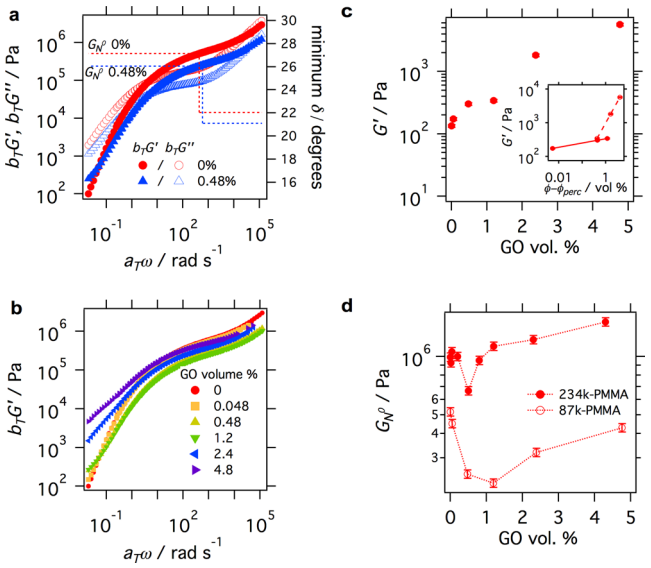

Figure 3. Rheological characterizations of PMMA/GO nanocomposites. (a) G' (solid symbols) and G'' (open symbols) of pure 87k-PMMA and 87k-PMMA/0.48 vol % GO composite as a function of frequency. (b) G' across the full concentration range studied for PMMA composites, as a function of frequency. (a) and (b) subject to TTS at a reference temperature of 200 °C. (c) Build up of G' with GO concentration at a fixed frequency of 0.02512 rad s^{-1} at a temperature of 200 °C for 87k- and 234k-PMMA composites. Inset shows application of a percolation model with G' as a function of the difference between GO vol % and percolation volume %. (d) The plateau modulus of the PMMA composites as a function of GO concentration.

In summary, this study of polymer−graphene oxide nanocomposites demonstrates that distortion of the polymer chains, due to the interfacial confinement effect from the high aspect ratio GO, reduces the number of interchain entanglements as measured using bulk rheology. We demonstrate that just 0.5% by volume of GO is enough to reduce the average chain dimensions in the bulk sample of poly(methyl methacrylate) by 12%, which highlights the potential for polymer−2D nanocomposites to produce changes in material properties with extremely economical use of nanofiller material. The link between the structural picture of the polymer chain confined at the interface with the dynamical rheological response, via a simple scaling argument based on simple thin-film polymer physics applied to a bulk situation, significantly advances our understanding of the mechanisms by which entangled polymer melts may be strongly altered by the presence of small quantities of high aspect ratio nanoparticles.

■ ASSOCIATED CONTENT

Supporting Information

The Supporting Information is available free of charge on the ACS Publications website at DOI: 10.1021/acsmacrolett.6b00100.

Experimental details: Composite preparation, SANS measurements, rheological measurements and additional interpretation, scaling analysis and correlation between $G_{N,SANS}^0$ and G_N^0 (PDF)

■ AUTHOR INFORMATION

Corresponding Author

*E-mail: weir.mp@gmail.com.

Author Contributions

∥These authors contributed equally to this work.

Notes

The authors declare no competing financial interest.

■ ACKNOWLEDGMENTS

EPSRC (UK) is acknowledged for supporting this work through grant reference number EP/K016784/1. STFC (UK) is acknowledged for provision of neutron scattering facilities though experiment number RB1410161. This work benefitted from SasView software, originally developed by the DANSE project under NSF award DMR-0520547. Professor Patrick Fairclough is acknowledged for use of equipment and for useful discussions. Dr. Adam Washington is acknowledged for assistance with SANS measurements. Professor Karen Winey is acknowledged for useful discussions.

■ REFERENCES

(1) Liu, F.; Ming, P.; Li, J. *Phys. Rev. B: Condens. Matter Mater. Phys.* **2007**, *76* (6), 064120.
(2) Liang, J.; Huang, Y.; Zhang, L.; Wang, Y.; Ma, Y.; Guo, T.; Chen, Y. *Adv. Funct. Mater.* **2009**, *19* (14), 2297−2302.
(3) Zhao, X.; Zhang, Q.; Chen, D.; Lu, P. *Macromolecules* **2010**, *43* (5), 2357−2363.
(4) Tung, W.-S.; Bird, V.; Composto, R. J.; Clarke, N.; Winey, K. I. *Macromolecules* **2013**, *46* (13), 5345−5354.
(5) Tuteja, A.; Duxbury, P. M.; Mackay, M. E. *Phys. Rev. Lett.* **2008**, *100* (7), 077801.
(6) Zhang, Q.; Archer, L. A. *Langmuir* **2002**, *18* (26), 10435−10442.
(7) See Supporting Information.
(8) Heenan, R. K.; Rogers, S. E.; Turner, D.; Terry, A. E.; Treadgold, J.; King, S. M. *Neutron News* **2011**, *22* (2), 19−21.

DOI: 10.1021/acsmacrolett.6b00100
ACS Macro Lett. 2016, 5, 430−434

(9) Pedersen, J. S. *Neutrons, X-Rays and Light, Chapter: Modelling of Small-Angle Scattering Data from Colloids and Polymer Systems*; Elsevier Science, 2002.
(10) Li, Y.; Wei, D.; Han, C. C.; Liao, Q. *J. Chem. Phys.* **2007**, *126* (20), 204907.
(11) Si, L.; Massa, M. V.; Dalnoki-Veress, K.; Brown, H. R.; Jones, R. A. L. *Phys. Rev. Lett.* **2005**, *94* (12), 127801.
(12) Sussman, D. M.; Tung, W.-S.; Winey, K. I.; Schweizer, K. S.; Riggleman, R. A. *Macromolecules* **2014**, *47* (18), 6462−6472.
(13) Nusser, K.; Schneider, G. J.; Richter, D. *Macromolecules* **2013**, *46* (15), 6263−6272.
(14) Schneider, G. J.; Nusser, K.; Willner, L.; Falus, P.; Richter, D. *Macromolecules* **2011**, *44* (15), 5857−5860.
(15) Li, Y.; Kröger, M.; Liu, W. K. *Phys. Rev. Lett.* **2012**, *109* (11), 118001.
(16) Crawford, M. K.; Smalley, R. J.; Cohen, G.; Hogan, B.; Wood, B.; Kumar, S. K.; Melnichenko, Y. B.; He, L.; Guise, W.; Hammouda, B. *Phys. Rev. Lett.* **2013**, *110* (19), 196001.
(17) Ashkar, R.; Abdul Baki, M.; Tyagi, M.; Faraone, A.; Butler, P.; Krishnamoorti, R. *ACS Macro Lett.* **2014**, *3* (12), 1262−1265.
(18) Bitsanis, I. A.; ten Brinke, G. *J. Chem. Phys.* **1993**, *99* (4), 3100.
(19) Stoller, M. D.; Park, S.; Zhu, Y.; An, J.; Ruoff, R. S. *Nano Lett.* **2008**, *8* (10), 3498−3502.
(20) Williams, M. L.; Landel, R. F.; Ferry, J. D. *J. Am. Chem. Soc.* **1955**, *77* (14), 3701−3707.
(21) Ramirez, J.; Likhtman, A. Reptate. Available from Reptate.com (accessed June 2014).
(22) Du, F.; Scogna, R. C.; Zhou, W.; Brand, S.; Fischer, J. E.; Winey, K. I. *Macromolecules* **2004**, *37* (24), 9048−9055.
(23) Kim, H.; Macosko, C. W. *Macromolecules* **2008**, *41* (9), 3317−3327.
(24) Graessley, W. W. *J. Polym. Sci., Polym. Phys. Ed.* **1980**, *18*, 27−34.
(25) Likhtman, A. E.; McLeish, T. C. B. *Macromolecules* **2002**, *35* (16), 6332−6343.
(26) Brown, H. R.; Russell, T. P. *Macromolecules* **1996**, *29* (2), 798−800.
(27) Lin, Y.-H. *Macromolecules* **1987**, *20*, 3080−3083.
(28) Fetters, L. J.; Lohse, D. J.; Richter, T. D.; Witten, T. A.; Zirkel, A. *Macromolecules* **1994**, *27* (17), 4639−4647.
(29) Liu, K.; Ronca, S.; Andablo-Reyes, E.; Forte, G.; Rastogi, S. *Macromolecules* **2014**, *48* (1), 131−139.

DOI: 10.1021/acsmacrolett.6b00100
ACS Macro Lett. 2016, 5, 430−434